frontiers | Frontiers in Built Environment

TYPE Original Research
PUBLISHED 15 February 2024
DOI 10.3389/fbuil.2024.1337986

OPEN ACCESS

EDITED BY
Yong Tan,
Tongji University, China

REVIEWED BY
Haizuo Zhou,
Tianjin University, China
Xianghua Song,
University of Jinan, China
Jian Ji,
Hohai University, China

*CORRESPONDENCE
Wei Guo,
guow@tju.edu.cn

RECEIVED 14 November 2023
ACCEPTED 31 January 2024
PUBLISHED 15 February 2024

CITATION
Yao H, Ma L, Duan Z and Guo W (2024), Reliability analysis of the cast-in-place bored pile with different defects.
Front. Built Environ. 10:1337986.
doi: 10.3389/fbuil.2024.1337986

Reliability analysis of the cast-in-place bored pile with different defects

Hua Yao[1], Lemin Ma[1], Zhiqiang Duan[2] and Wei Guo[2]*

[1]Tianjin Survey Design Institute Group Co, Ltd., Tianjin, China, [2]School of Civil Engineering, Tianjin University, Tianjin, China

The defects of the cast-in-place bored piles heavily influence their integrities and bearing capacities. The bearing capacity and reliability index of the cast-in-place bored piles with different defects were studied using the finite element method. The accuracy of the numerical model is verified by the field test results of an *in situ* cast-in-place bored pile. Parametric studies are conducted to investigate the toe debris, mud cake, and necking and bulging defects on the ultimate bearing capacities of the cast-in-place bored piles. The results indicate that maximum reduction in the ultimate bearing capacities of the cast-in-place bored pile was observed, with the ultimate bearing capacity of the toe debris defect decreased by 17%, that of the mud cake defect decreased by 19%, that of the necking defect by 6.1%, and that of the pile bulging defect increased by 40.9%. The minimum reliability index can be 0.81 when the diameter of the pile necking defect is 0.2 m. The maximum reliability index can be 3.63 when the diameter of the pile necking defect is 2.0 m.

KEYWORDS

cast-in-place bored pile, reliability, pile defects, bearing capacity, finite element method

1 Introduction

The cast-in-place bored piles are extensively used as the foundation for high-rise buildings because of their high bearing capacity (Zhang et al., 2013; Kou et al., 2016). However, the pile defects in the pile body, i.e., toe debris, mud cake, and necking and bulging defects, heavily affect its integrity and bearing capacity, which have been investigated by many researchers through field tests (Jiang et al., 2004), centrifuge tests (Wong, 2004), numerical analyses (Chen, et al., 2001; Fu et al., 2015; Huang, 2018; Yuan et al., 2018), and theoretical studies (Zhang et al., 2022).

The existence of toe debris at the bottom of the cast-in-place bored piles not only affects their tip resistance but also reduces their side resistance. It is found that the ultimate bearing capacity of a single pile reduced by 11%–25% due to a thick toe debris at the bottom of the pile (Wu and Wang, 2009). The finite element analyses conducted by Guan et al. (2021) found that the ultimate bearing capacity of the pile foundation enhances with the increase of the elastic modulus and internal friction angle of the toe debris but is affected less by its cohesion. The bearing capacity changes steadily with the increase in the thickness of the toe debris, with a critical value ranging from 35 cm to 45 cm, after which the tip resistance was determined using the properties of the toe debris with no relationship to the bearing soil layer (Hu et al., 2014).

A mud cake may be formed on the surface of the cast-in-place bored pile due to mud wall protection during pile construction (Zhang et al., 2006; Yang et al., 2009). A thicker mud cake reduces the side friction between the cast-in-place bored pile and surrounding soil (Wu, 2010;

Yang, 2011; Qi et al., 2015). The shear tests show that the interface friction angles between the pile and soil were reduced by approximately 40% (Yang et al., 2009; Li et al., 2015; Chen et al., 2018; Li et al., 2022). The effect of the mud cake is related to pile types, especially for friction piles (Zhang et al., 2006; Yang et al., 2009; Wang et al., 2014). The thicker the mud cake, the weaker the interactions between the cast-in-place bored pile and the surrounding soil (Yu et al., 2006; Zhou, 2007; Wu, 2010; Yang, 2011).

The necking and bulging defects of the cast in place bored piles heavily influence their ultimate bearing capacity (Poulos, 2005; Wang et al., 2014; Zheng et al., 2018; Zhou, 2020; Cui et al., 2023). Pile necking is a common defect in the construction of cast-in-place bored pile foundations induced by water loss, mud cake, and soft clay fall into a drilled hole. Pile necking can induce a serious integrity problem and affect its bearing capacity (Zhang, 2005b). The bulging defect is often due to foreign materials in the concrete pile. Although it can increase the load capacity, the cast-in-place bored pile is still considered a defect. Numerical analysis and model tests showed that the shallower the pile shrinkage is, the greater the effect on pile settlement and internal force (Wang and An, 2011; Qian et al., 2020a; 2020b; Fang et al., 2020).

The reliability analyses of the cast-in-place bored piles mainly focused on the evaluation of their failure probability due to the abovementioned defects. The commonly used probability analyses include the first-order second-moment method (FOSM); a method recommended by the Joint Committee on Structural Safety (JCSS), the so-called JC method; and the method that involves a combination of the support vector machine (SVM) and the first-order reliability method (FORM). The basic principle of the FOSM is to expand the utility function at a point in the failure surface with a Taylor series and take a primary term considering the actual distribution of random variables. The mean value and standard deviation of the random variables are used to solve the reliability index. The FOSM is widely used to calculate the reliability index of the pile with different defects based on the limit state function (Samman et al., 1997; Li et al., 2008; Ji et al., 2019; Ji et al., 2023). The JC method is based on the FOSM in dealing with arbitrarily distributed random variables by transforming the random variable with a non-normal distribution into a random variable with normal distribution. The JC method is often used to calculate the reliability index of the toe debris, necking, and bulging defects of piles (Zhang et al., 2005a; Zhang et al., 2005c). The method that combines the support vector machine and the FORM was used to calculate the reliability index of piles with necking defects by Xu et al. (2022). The optimized SVM model is obtained by training a simple utility function using an SVM in machine learning.

In this paper, numerical studies are conducted to investigate the performance of the cast-in-place bored piles with the assumed defects of toe debris, mud cake, necking, and bulging. The accuracy of the numerical model is verified by the field test results of an *in situ* cast-in-place bored pile. Parametric studies are conducted to investigate the defects of toe debris, mud cake, and necking and bulging on the ultimate bearing capacities and the reliability index of the cast-in-place bored piles. Unlike considering a particular defect alone, the influence of the four types of defects on the bearing capacity of the cast-in-place bored piles is quantitatively studied. The reliability analyses considering the uncertainties of the four defects are investigated based on results of 108 field tests.

2 Case history

A super high-rise building with a total height of 530 m was constructed in Tianjin, China. It was designed to use 1,262 cast-in-place bored piles and a raft foundation to support the high-rise building. Each cast-in-place bored pile had an outer diameter of 0.8 m and different depths ranging from 30 to 52.7 m. The selected three piles, as shown in Figure 1, named as KYZ-1, KYZ-2, and KYZ-3, were loaded to measure their bearing capacity with their pile lengths of 52.5 m, 52.4 m, and 52.3 m, respectively.

The soil types in the site were generally consistent with their distribution profiles, as shown in Figure 2. It could be roughly divided into three layers: the surface layer (above 5.4 m), the intermediate layer (from 5.4 to 29.4 m), and the bottom layer (below 29.4 m). The surface layer consisted of backfills, clay, and silty clay, with a depth of 5.4 m. The stratum ranging from 2.0 to 3.5 m is dominated by clay with high compressibility. The intermediate layer includes clay, silty clay, and silt, with a total depth of 25 m. The stratum ranging from 5.4 to 16.6 m mainly consists of mud and mucky clay and has low strength, poor soil quality, and high water content, with its undrained shear strength ranging from 12.9 to 17.0 kPa. This layer of the soil was generally normally consolidated with its undrained shear strength ranging from 50 to 400 kPa. The bottom layer consisted of predominantly silty clay, clay, and sand layers. The soil properties of each sub-layer are uniform but are uneven horizontally distributed. The sand layer below 52.2 m from the ground surface has an undrained shear strength of 498 kPa and was selected as the bearing layer of the cast-in-place bored piles. The depth of the water table in the area ranges from 1.5 to 2 m. More details on the soil properties of the site are summarized in Table 1.

The pile load test was carried out after pile installation in accordance with the China Technical specification for Testing of Building Foundation Piles (JGJ106-2003) (MCC, 2003). The reaction system composed of the anchor pile, bearing platform, and reaction beams was used to supply the reaction force. Two hydraulic jacks with their loading capacities of 5,000 kN were used to apply the vertical axial loads. Four LVDTs with a measuring range of 50 mm were used to record the settlement of the pile surface. The load was applied in step of 700, 1,400, and 7,000 kN with loading step of approximately one-tenth of their ultimate loading capacity. The vertical displacement of the pile was measured for the first 5, 15, 30, 45, and 60 min at each load step and then once every 30 min. The difference between displacements at 30 min and 1 h after the application of each load increment was calculated. If this difference was less than 0.1 mm, then the next load increment was applied. If the displacement at the pile cap was more than five times, the displacement at the beginning of the load increment or the displacement did not stabilize after 24 h of loading; loading was discontinued.

The comparison of the applied load versus settlement curves of the field test piles is shown in Figure 3. It can be found that the cast-in-place bored piles were not destroyed after the final loading of 7,000 kN. The final settlements of the pile nos. KYZ-1, KYZ-2, and KYZ-3 were 8.27, 7.78, and 10.23 mm, respectively. The ultimate bearing capacity of the piles Q_{uf} is determined using the tangential intersection method proposed by Charles et al. (1988). The intersection of the two tangential lines of the gentle part and the

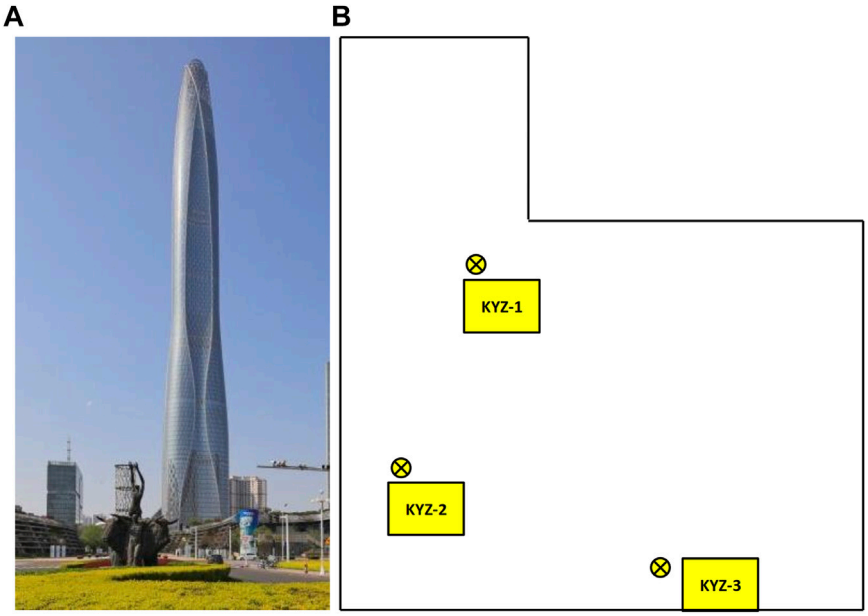

FIGURE 1
Location of the field test; **(A)** site photo and **(B)** locations of KYZ-1, KYZ-2, and KYZ-3.

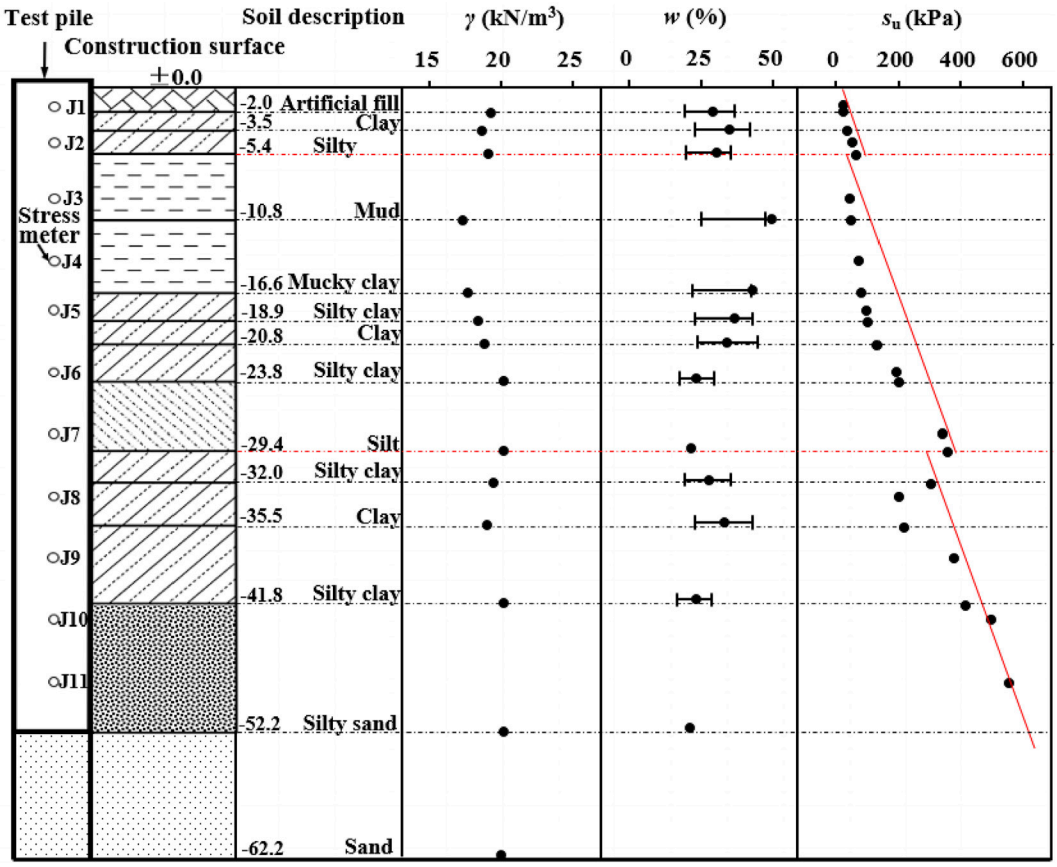

FIGURE 2
Graphic profile and stress meter location map.

TABLE 1 Soil properties of the site.

Soil type	Thickness (m)	c (kPa)	φ (°)	V_s (m/s)	E (MPa)	ν
Fill layer	2	35	3	116	36	0.35
Clay	1.5	33	2.1	144.0	53	
Silty clay	2	20.8	35	158.1	66	
Mud	5.3	12	0.5	121.4	35	
Muddy clay	5.8	18.4	0.5	155.1	59	
Silty clay	2.3	35.2	1.8	166.3	70	
Clay	1.9	49.8	1.9	227.7	134	
Silty clay	3	53	0.6	251.8	176	
Silt	5.6	59.8	35	310.6	239	
Silty clay	2.6	51	2.5	276.0	205	
Clay	3.5	48.5	1.3	273.3	195	
Silty clay	6.3	67.8	2	273.3	208	
Silt sand	10.4	16.6	36.2	392.1	412	0.30
Sand	57.8	20.6	37.7	407.9	400	

end part of the *Q*–*S* curve is taken as the ultimate bearing capacity. The obtained ultimate bearing capacity Q_{uf} of pile nos. KYZ-1, KYZ-2, and KYZ-3 is 4,800, 4,880, and 4,690 kN, respectively.

3 Numerical method

The commercial software ABAQUS is used to simulate the bearing capacity of the *in situ* cast-in-place bored pile nos. KYZ-1, KYZ-2, and KYZ-3 with their lengths L_p of 52.5 m, 52.4 m, and 52.3 m, respectively. The soil foundation is simulated as the axisymmetric finite element model with a height of 110 m or almost two times the pile length, as shown in Figure 4. The Mohr–Coulomb model is adopted to simulate the soil material using the four-node bilinear axisymmetric quadrilateral (CAX4R) element. The soil mesh near the pile is encrypted to reflect the large deformation gradient.

The pile is simulated as the linear elastic model using the four-node bilinear axisymmetric quadrilateral element. The unit weight, Young's modulus, and Poisson's ratio of the concrete material used for the pile were 25 kN/m^3, 30 GPa, and 0.25, respectively. The other properties of the three-pile models are shown in Table 2. The left and right boundaries are allowed to move freely in the vertical direction but fixed in the horizontal direction. The bottom boundary is fixed in both directions. The numerical analysis was divided into the following two steps: 1) build the initial equilibrium between gravity, hydraulic pressure, and deformation of soil and 2) apply a vertical load using the steps discussed in Section 2.

The load–settlement curves from the numerical studies and *in situ* loading tests are shown in Figure 3. The ultimate bearing capacities of the three pile models calculated from the load–settlement curves from *in situ* tests, Q_{uf}, and that from numerical studies, Q_{un}, are further summarized in Table 2. It can be found that the two results fairly match each other, with the difference between the two sets of results of less than 8.04%.

4 Results and discussion

4.1 Numerical results

Numerical studies are conducted to investigate the effect of the toe debris, mud cake, and necking and bulging defects on the bearing capacity of the cast-in-place bored piles with a length of 52.5 m and a pile diameter of 0.8 m. The numerical model and parameters used are the same as those discussed in Section 2. The parameters used in the parametric studies are summarized in Tables 3–6. The sketch illustrating the types of the defects is shown in Figure 5.

The cast-in-place bored pile is simulated to study the effect of toe debris thicknesses on the ultimate bearing capacity of the cast-in-place bored pile, as shown in Figure 6A. The elastic modulus *E* and internal friction angle φ of the cast-in-place bored piles are taken as 5 MPa and 30°, respectively, and different toe debris thicknesses ranging from 3 cm to 30 cm are simulated as shown in Table 3. The ultimate bearing capacities of the pile non-linearly decrease with the thickness of the toe debris. When the toe debris thickness is larger than 10 cm, the ultimate bearing capacity remains almost constant because it is determined by the side resistance at the condition. The effects of the elastic modulus of the toe debris on the ultimate bearing capacity of the cast-in-place bored piles are shown in Figure 6B. The elastic modulus of the toe debris ranges from 5 to 40 MPa, and the thickness and internal friction angle of the cast-in-place bored pile are taken as 3 cm and 30°, respectively. As expected, the ultimate bearing capacity of the pile non-linearly increases with the increase in the elastic modulus of the toe debris. The effects of the internal friction angle of the toe debris on the ultimate bearing capacity of the cast-in-place bored piles are shown in Figure 6C. The internal friction angle of the toe debris ranges from 10° to 20°, and the thickness and the elastic modulus of the cast-in-place bored pile are taken as 3 cm and 5 MPa, respectively. It is found that the internal friction angles have a

10.3389/fbuil.2024.1337986

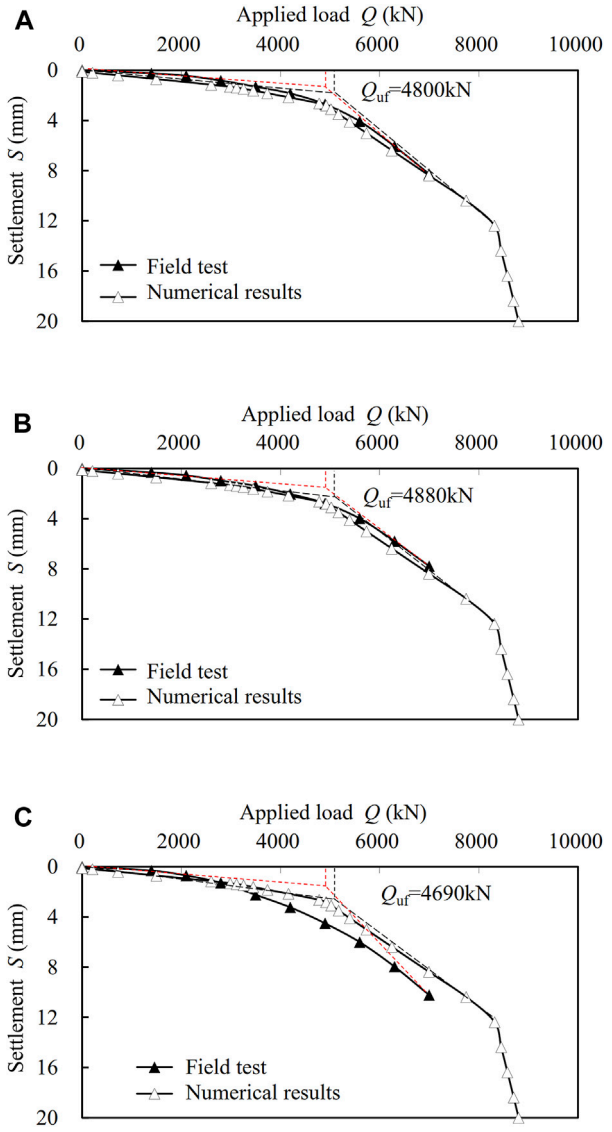

FIGURE 3
Comparison of the load–settlement curves between the field test and the finite element analysis of the cast-in-place pile **(A)** KYZ-1, **(B)** KYZ-2, and **(C)** KYZ-3.

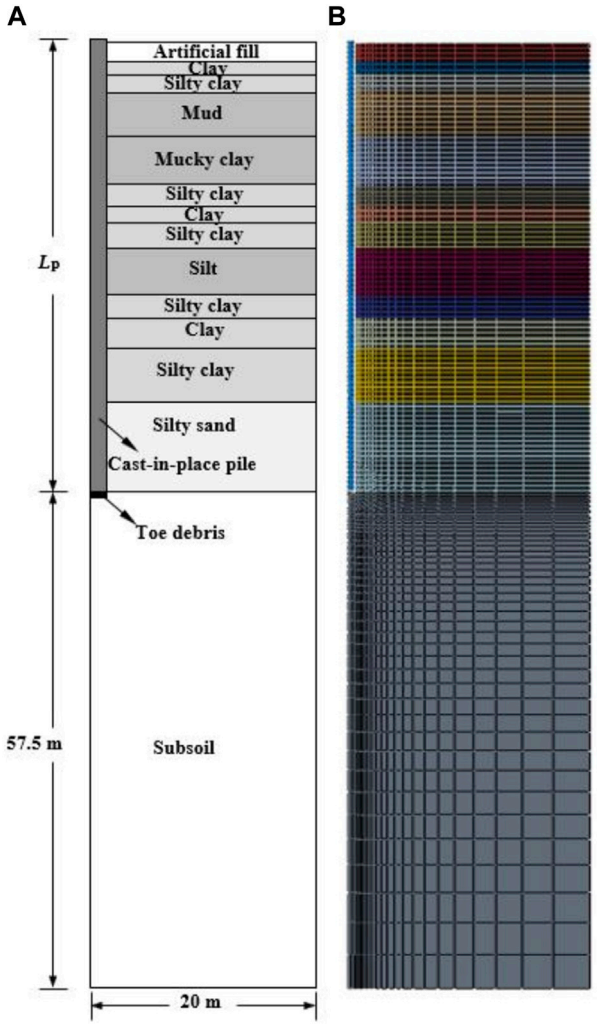

FIGURE 4
Finite element model for the cast-in-place pile: **(A)** geometric model; **(B)** axisymmetric finite element model.

little effect on the ultimate bearing capacity of the cast-in-place bored piles.

The effect of the thicknesses, t_m, of the mud cake on the ultimate bearing capacity of the cast-in-place bored pile is shown in Figure 7A. The cast-in-place bored piles are simulated, with the internal friction angle φ and the cohesion c of the cast-in-place bored piles taken as 20° and 18 kPa, respectively; different mud cake thicknesses ranging from 1 cm to 8 cm are simulated as shown in Table 4. Generally, the ultimate bearing capacity of the cast-in-place bored piles non-linearly decreases with the increase in the thickness of the mud cake. The ultimate bearing capacity of the pile decreases sharply with the appearance of the mud cake, and it then tends to be flat. The effects of the internal friction angle of the mud cake on the ultimate bearing capacity of the cast-in-place bored pile are shown in Figure 7B. The internal friction angle of the mud cake ranges from 5° to 20°, and the thickness and cohesion of the cast-in-place bored piles are taken as 1 cm and 18 kPa, respectively. With the increase of the internal friction angle, the ultimate bearing capacity of the cast-in-place bored piles approximately linearly increases. The effects of the cohesion of the mud cake on the ultimate bearing capacity of the cast-in-place bored pile are shown in Figure 7C. The cohesion of the mud cake ranges from 6 to 24 kPa, and the thickness and the internal friction angle of the cast-in-place bored piles are taken as 1 cm and 20°, respectively. With the increase in the cohesion of the mud cake, the ultimate bearing capacity of the cast-in-place bored piles non-linearly increases. When the mud cake cohesion increases over 18 kPa, the ultimate bearing capacity of the pile tends to be stable.

The effects of pile necking and bulging defects on the ultimate bearing capacity of the cast-in-place bored pile are observed based on the parameters of the numerical model of the KYZ-1 pile. As shown in Figure 8A, the diameter of pile necking defects D_n ranging from 0.2 m to 0.6 m and different diameters of pile bulging defects ranging from 1.2 m to 2.0 m are simulated to investigate their effect on the ultimate bearing capacity of the cast-in-place bored pile. The

TABLE 2 Construction parameter of the cast-in-place pile.

Pile no.	Dimension (mm × m)	Final loading (kN)	Final settlement (mm)	Q_{uf}/kN	Q_{un}/kN	Difference %
KYZ-1	Φ800 × 52.5	7,000	8.27	4,800	4,890	1.84
KYZ-2	Φ800 × 52.4	7,000	7.78	4,880	5,020	2.79
KYZ-3	Φ800 × 52.3	7,000	10.23	4,690	5,100	8.04

TABLE 3 Parameters used in the parametric studies to consider the toe debris defects.

Type of defect	t_d (cm)	E (MPa)	φ (°)	c (kPa)	ν
Toe debris defect	3	5	30	2	0.3
	5				
	10				
	20				
	30				
	3	5	30	2	0.3
		10			
		20			
		40			
	3	5	10	2	0.3
			20		
			30		

TABLE 4 Parameters used in the parametric studies to consider the mud cake defects.

Type of defect	t_m (cm)	φ (°)	c (kPa)	E (MPa)	ν
Mud cake defect	1	20	18	5	0.3
	2				
	4				
	8				
	1	5	18	5	0.3
		10			
		15			
		20			
	1	20	6	5	0.3
			12		
			18		
			24		

length of the defects L_n is 3 m, and the depth of the defects is 26 m from the ground surface, as shown in Table 5. The ultimate bearing capacity decreases with the decrease of the diameter of the pile

TABLE 5 Parameters used in the parametric studies to consider the necking defects.

Type of defect	D_n (m)	L_n (m)	H_n (m)
Necking defect	0.2	3.0	26
	0.4		
	0.6		
	0.4	1.0	26
		2.0	
		3.0	
	0.4	3.0	13
			26
			39

TABLE 6 Parameters used in the parametric studies to consider the bulging defects.

Type of defect	D_b (m)	L_b (m)	H_b (m)
Bulging defect	1.2	3.0	26
	1.6		
	2.0		
	1.6	1.0	26
		2.0	
		3.0	
	1.6	3.0	13
			26
			39

necking defects when the length and depth remain unchanged. The ultimate bearing capacity increases with the increase in the diameter of pile bulging defects when the length and depth remain unchanged. The effects of the length of pile necking L_n and bulging defects on the ultimate bearing capacity of the cast-in-place bored pile are shown in Figure 8B. The diameters of 0.4 m and 1.6 m at the depth of 26 m from the ground surface for the pile necking defect and pile bulging defects and the different lengths of the pile necking and bulging defects ranging from 1.0 m to 3.0 m are simulated. As expected, the ultimate bearing capacity of the piles linearly decreases with the length of the pile necking defects and linearly increases with the length of the pile bulging defects. Compared with the integrated pile, the ultimate bearing capacity

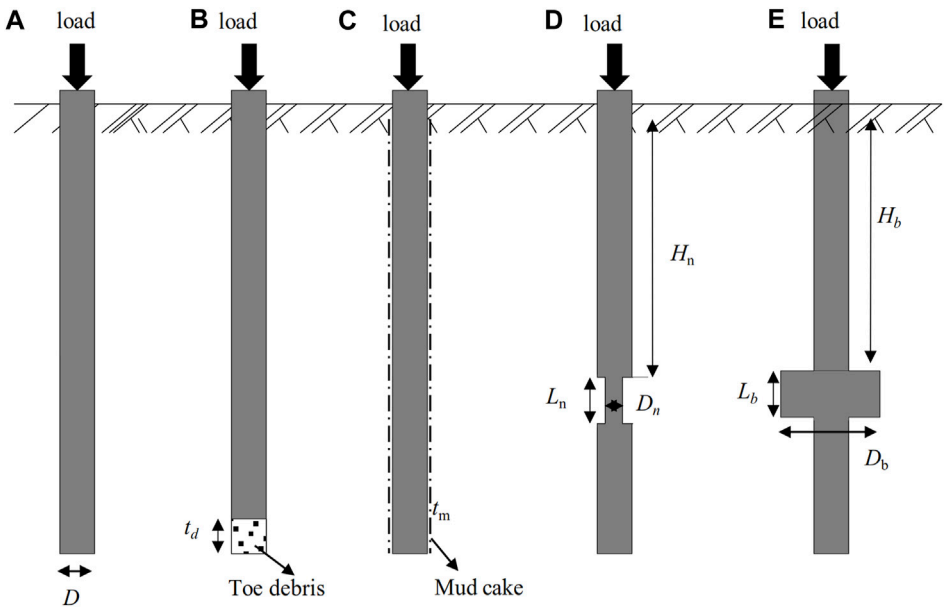

FIGURE 5
Parameter analysis diagram of the defective pile, **(A)** normal pile, **(B)** toe debris defect, **(C)** mud cake defect, **(D)** necking defect, and **(E)** bulging defect.

of the pile necking defect can be reduced by 6.1%, while that with the pile bulging defect can increase by 40.9%. This is because the pile bulging defect transfers the load to the lower soil mass which plays the role of "prestress" during the stress process (Qian, 2004). As shown in Figure 8C, the depth of the pile necking H_n and bulging H_b defects ranging from 13 m to 39 m is simulated to investigate their effect on the ultimate bearing capacity of the cast-in-place bored pile, when the diameters of the pile necking and bulging defects are 0.4 m and 1.6 m, and their length is 3.0 m. Generally, the greater the depth of pile necking and bulging defects, the higher the ultimate bearing capacity of the pile. When the depth of the defects increases from 13 m to 39 m, the ultimate bearing capacity of the pile necking and bulging defects increases by 7.4% and 16.9%, respectively.

4.2 Reliability analysis

Reliability analyses are conducted to reflect the safety of the cast-in-place bored piles with toe debris, mud cake, necking, and bulging defects. Load effect combinations are considered only for the dead load and live load, and the integrated pile is analyzed with the dimensionless limit-state equations, calculated as follows (Zheng et al., 2010):

$$g(\lambda_R, \lambda_{RF}, \lambda_{QD}, \lambda_{QL}) = \lambda_{RD} - m\lambda_{QD} - \rho m\lambda_{QL} = 0, \quad (1)$$

$$\lambda_{RD} = \lambda_{RF} \cdot \lambda_R, \quad (2)$$

$$\mathrm{COV}_{RD} = \sqrt{\mathrm{COV}_R^2 + \mathrm{COV}_{RF}^2}, \quad (3)$$

where λ_R is the bias factor of the bearing capacity; λ_{RF} is the bias factor of the reduction factor RF; λ_{RD} is the bias factor of the bearing capacity of the pile with defects; λ_{QD} and λ_{QL} are the bias factors of the dead load and live load, respectively; ρ is the ratio of the live load to dead load; m is a fixed value and $m = 1/F_s(1+\rho)$; RF is the reduction factor used to evaluate the bearing capacity of a single pile with defects and $RF = Q_i/Q_d$ (Poulos, 2005); Q_i is the bearing capacity of the integrated pile; Q_d is the bearing capacity of the pile with defects; COV_{RD} is the coefficient of variation of the bearing capacity of the pile with defects; COV_R is the coefficient of variation of the bearing capacity; COV_{RF} is the coefficient of variation of the reduction factor RF.

The reliability index β has been derived by FHWA (1998) for reliability analyses of the axial driven pile. Replacing λ_R with λ_{RD} in the original equation gives the reliability index β of the defective piles as

$$\beta = \frac{\ln\left[\left(\frac{\lambda_{RD}F_S(Q_D/Q_L+1)}{\lambda_{QD}Q_D/Q_L+\lambda_{QL}}\right)\sqrt{\frac{1+\mathrm{COV}_{QD}^2+\mathrm{COV}_{QL}^2}{1+\mathrm{COV}_{RD}^2}}\right]}{\sqrt{\ln\left[(1+\mathrm{COV}_{RD}^2)\left(1+\mathrm{COV}_{QD}^2+\mathrm{COV}_{QL}^2\right)\right]}}, \quad (4)$$

where F_S is the factor of safety; Q_D and Q_L are the values of dead load and live load, respectively; COV_{QD} and COV_{QL} are the coefficients of variation of dead load and the live load, respectively.

The reliability index β of defective piles is calculated using the parameters given in the AASHTO specification (AASHTO, 1998), such as $\lambda_{QD} = 1.08$, $\lambda_{QL} = 1.15$, $\mathrm{COV}_{QD} = 0.13$, $\mathrm{COV}_{QL} = 0.18$, $Q_D/Q_L = 2.0$, and $F_s = 2.0$. As shown in Figure 9, the statistical results of the ratio between the test and the calculated value of the bearing capacity are presented based on the data of the bored piles in the field test. The bias factor and coefficient of variation of the bearing capacity are $\lambda_R = 0.8263$ and $\mathrm{COV}_R = 0.0229$, respectively. Due to the limited data of the numerical analysis, the value of λ_{RF} approximates the reduction factor RF of pile with defects in the parametric analysis, and COV_{RF} is taken as 0.1 to quantify the effect of defects on the coefficient of variation (Li et al., 2008). The bias factor λ_{RD} of the bearing capacity of the pile with defects is obtained by substituting λ_{RF} with λ_R in Eq. 2.

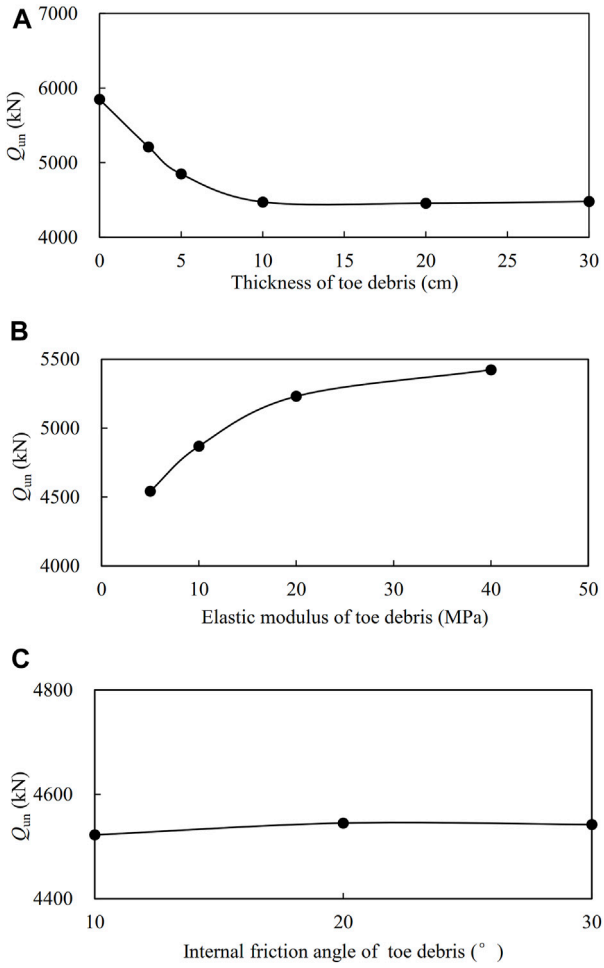

FIGURE 6
Effects of toe debris on the ultimate bearing capacity of the cast-in-place bored pile: **(A)** thickness, **(B)** elastic modulus, and **(C)** internal friction angle.

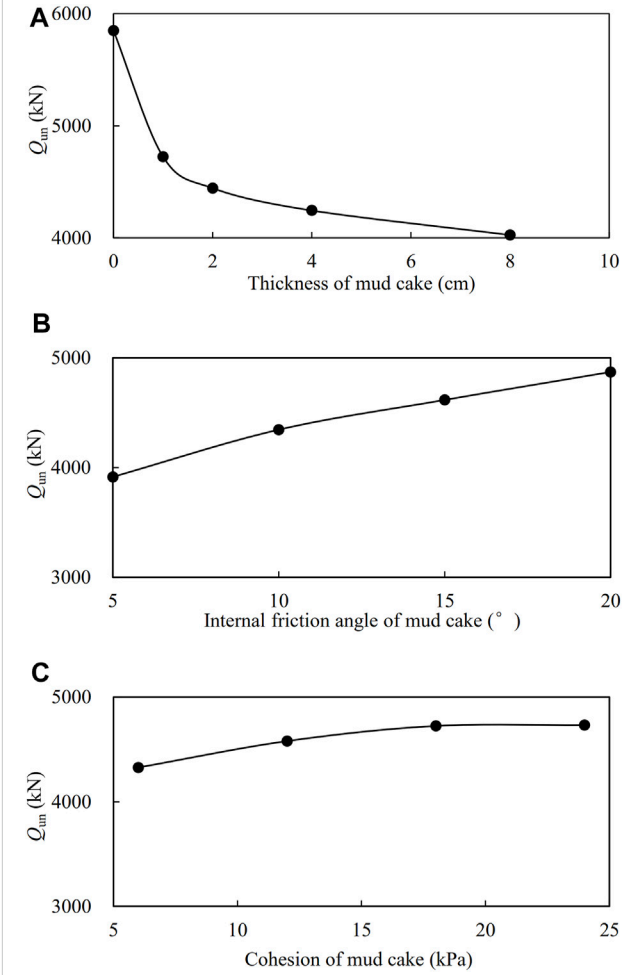

FIGURE 7
Effects of the mud cake on the ultimate bearing capacity of the cast-in-place bored pile: **(A)** thickness, **(B)** internal friction angle, and **(C)** cohesion.

The coefficient of variation of the bearing capacity of the pile with defects, COV_{RD} = 0.103, is obtained by substituting the COV_R and COV_{RF} in Eq. 3. Substituting the above parameter values into Eq. 4 yields a reliability index for the bearing capacity of the pile with defects.

The bearing stability of the cast-in-place bored piles with defects such as the pile toe debris, pile mud cake, necking, and bulging diameter is further studied with their reliability index analyzed. The influence of the toe debris defect on the reliability index of the cast-in-place pile is shown in Figure 10A. It can be found that the thickness t_m and elastic modulus E of toe debris have significant effects on the reliability index, while the internal friction angle φ has little effects on the reliability index β. When the thickness of toe debris increases from 3 cm to 30 cm, the reliability index of the toe debris pile reduces from 1.36 to 0.62. When the elastic modulus E of the toe debris increases from 5 MPa to 40 MPa, the reliability index of the toe debris pile increases from 0.72 to 1.54. It shows that when the toe debris reaches a certain thickness or the strength of the soil is very weak, the reliability index gradually approaches a fixed value, and the toe debris pile has no pile end resistance and becomes a friction pile. For different internal friction angles, the reliability index basically keeps constant and is close to 0.7.

The influence of the mud cake defect on the reliability index of the cast-in-place pile is shown in Figure 10B. It can be found that the thickness t_m and the elastic modulus E of the mud cake parameters have a significant impact on the reliability index of the cast-in-place bored piles. When the thickness of the mud cake t_m increases from 1 cm to 8 cm, the reliability index of the mud cake pile decreases from 0.90 to 0.16. The internal friction angle φ of the mud cake has a notable effect on the reliability index of the mud cake pile. The internal friction angle increases from 5° to 20°; the reliability index increases from 0.03 to 1.04. Similarly, cohesion has a great effect on the reliability index, and the reliability index increases from 0.49 to 1.91 when the cohesion ranges from 6 kPa to 24 kPa. This is because the properties of the mud cake affect the interaction between the pile and soil and further affect the side friction resistance and ultimate bearing capacity of the pile.

It can be found from Figure 10C that when the length L_n and depth D_n of the pile necking defect are constant, the reliability index changes from a slow change to a steep change with the decrease of the diameter D_n of pile necking defects. It can be found that the reliability index increases sharply when the

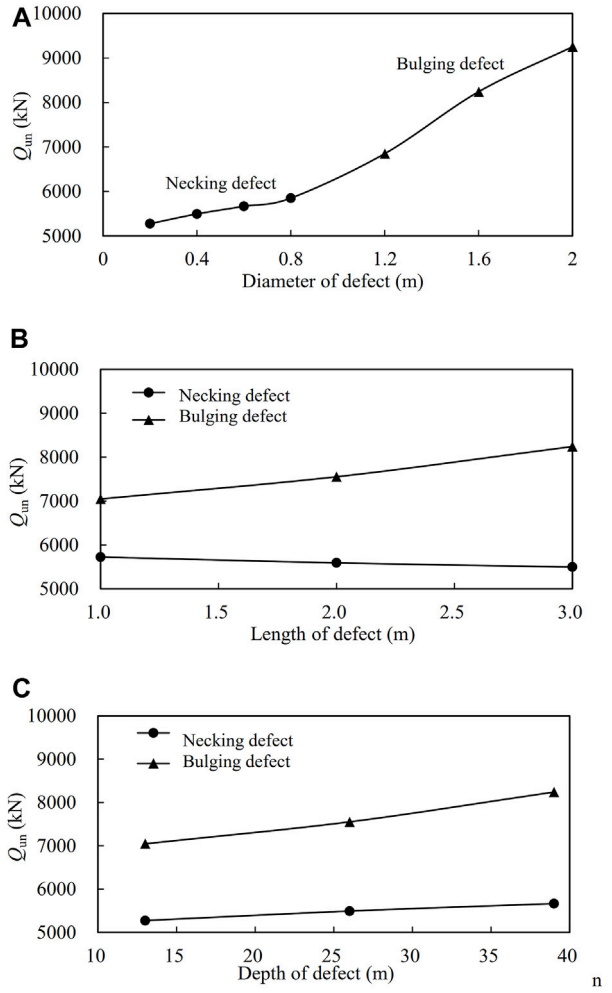

FIGURE 8
Effects of necking and bulging defects on the ultimate bearing capacity of the cast-in-place bored pile: **(A)** diameter of defects; **(B)** length of defects, H_n = H_b = 26 m; and **(C)** depth of defects L_n = L_b = 3 m.

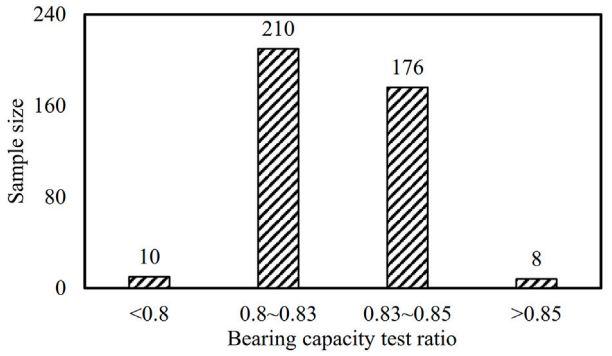

FIGURE 9
Test ratio of the bearing capacity of the pile in the field test.

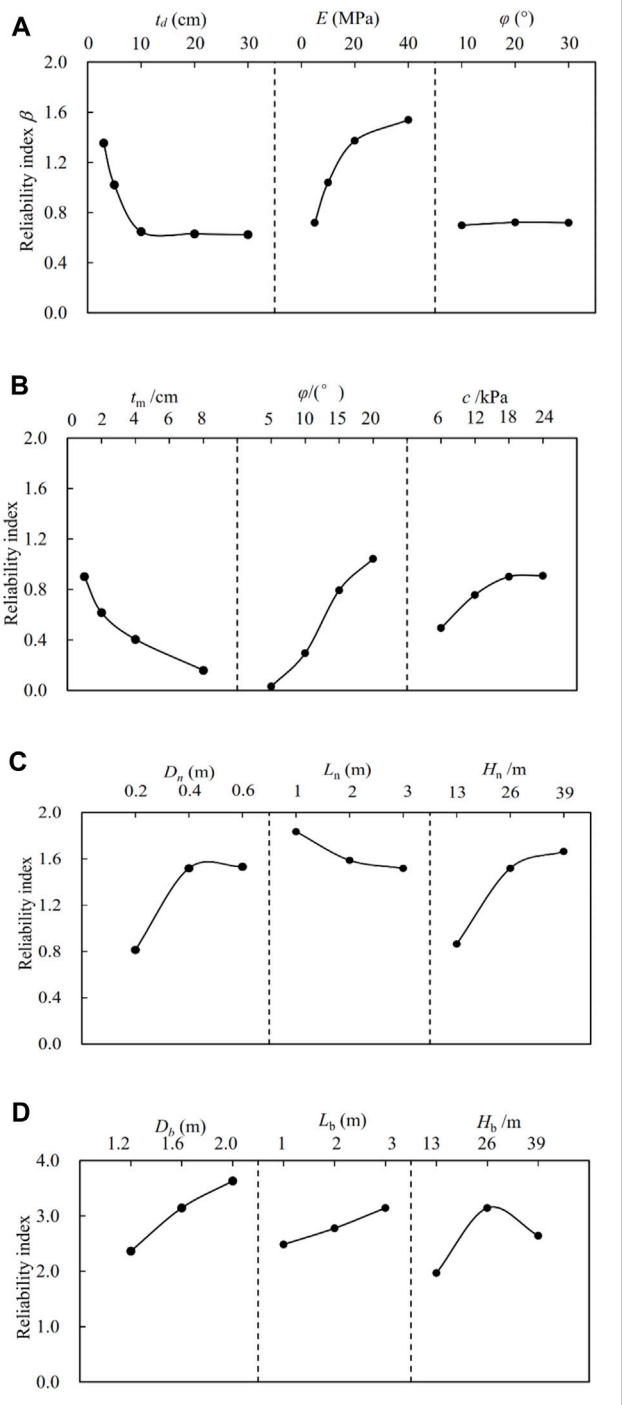

FIGURE 10
Influence of the defects on the reliability index of the cast-in-place bored pile: **(A)** toe debris defect, **(B)** mud cake defect, **(C)** necking defect, and **(D)** bulging defect.

diameter of the pile necking defect is less than 0.4 m. This is because the stress at the pile necking defect is too great, which leads to the fracture of the pile body. The reliability index decreases slowly with the increase in the length of the pile necking defect, ranging from 1.84 to 1.52. One of the possible reasons may be the increase in the length of the pile necking defect, which reduces the side friction resistance of the pile, and the decrease of the ultimate bearing capacity of the pile. The maximum value of the pile side friction occurs at 1/3 pile length from the loaded position. When the pile necking defect is close to 1/3 pile length from the surface or H_n = 13 m, the

more loss of the pile side friction and the smaller the reliability index. When the pile necking defect is far away from the surface, H_n = 26 m and 39 m, the necking location has little effect on the reliability index.

The influence of the bulging defect on the reliability index of the cast-in-place bored pile is shown in Figure 10D; the reliability index obviously increases with the increase of the pile bulging size. This is because the surrounding soil is compacted due to pile bulging, which increases the ultimate bearing capacity of the pile foundation. The reliability index increases with the increase in the bulging length H_b. This is because the increase in the length of the pile bulging defect is conducive to the development of pile side resistance. The reliability index increases first and then decreases with the increase in the depth of the pile bulging defect. Generally, when the bulging pile is a failure, the soil on the pile bulging defect will be separated from the pile and the side friction resistance of the pile will be reduced.

5 Conclusion

The finite element method was used to analyze the bearing characteristics of the piles under different defects. Parametric studies are conducted to investigate the toe debris, mud cake, necking, and bulging defects on the ultimate bearing capacities and the reliability index of the cast-in-place bored piles. The following conclusions can be drawn from the current studies:

1) Compared with the integrated pile, the ultimate bearing capacity loss of a single pile caused by toe debris is 17%. The ultimate bearing capacity and reliability index of the pile with toe debris decrease significantly with the increase in the toe debris thickness. When the toe debris thickness exceeds 10 cm, the reliability index is only 0.7. The reliability index of the toe debris pile increases with the increase of the elastic modulus of toe debris. When the elastic modulus of toe debris reaches 40 MPa, the reliability index gradually changes. The reliability index is insensitive to the change in the internal friction angle, which is close to 0.7.
2) The ultimate bearing capacity and reliability index of the pile sharply decrease with the mud cake defect. When the mud cake thickness is 1 cm, the ultimate bearing capacity of the pile decreases to 19.2% of that of the integrated pile with its reliability index of 0.90. The reliability index decreases with the increase in the mud cake thickness and also increases with the increase in the internal friction angle and cohesion.
3) The necking defects decrease the ultimate bearing capacity and reliability index of the pile. The minimum reliability index was 0.81 when the diameter of the pile necking defect is 0.2 m. The ultimate bearing capacity and reliability index of the pile are reduced with the decrease in the diameter and the depth of the pile necking defects and the increase in the length of the pile necking defects.
4) The bulging defects improve the ultimate bearing capacity and reliability index of the cast-in-place pile, with the maximum reliability index of 3.63 and the diameter of the pile bulging defect of 2.0 m. The ultimate bearing capacity of the pile increases with the increase in the diameter and the length of the pile bulging defects. However, the reliability index increases first and then decreases with the increase in the depth of the pile bulging defect.

Data availability statement

The original contributions presented in the study are included in the article/Supplementary material; further inquiries can be directed to the corresponding author.

Author contributions

HY: Data curation, Investigation, Software, Writing–original draft, Writing–review and editing. LM: Conceptualization, Data curation, Investigation, Writing–original draft, Writing–review and editing. ZD: Conceptualization, Data curation, Investigation, Methodology, Writing–original draft, Writing–review and editing. WG: Formal Analysis, Funding acquisition, Investigation, Supervision, Validation, Writing–review and editing.

Funding

The author(s) declare that no financial support was received for the research, authorship, and/or publication of this article.

Conflict of interest

HY and LM were employed by Tianjin Survey Design Institute Group Co., Ltd.

The remaining authors declare that the research was conducted in the absence of any commercial or financial relationships that could be construed as a potential conflict of interest.

The reviewer HZ declared a shared affiliation with the author WG to the handling editor at the time of review.

The author(s) declared that they were an editorial board member of Frontiers, at the time of submission. This had no impact on the peer review process and the final decision.

Publisher's note

References

AASHTO (1998). *LRFD bridge design specifications: SI units*. 2. Washington, D.C: American Association of State Highway and Transportation Officials.

Charles, H., Trautmann, F., and Kulhawy, H. (1988). Uplift load-displacement behavior of spread foundations. *J. Geotech. Engrg.* 114 (2), 168–184. doi:10.1061/(asce)0733-9410(1988)114:2(168)

Chen, B., Zhuo, J. S., and Zhou, L. J. (2001). Finite element analysis of the vertical bearing capacity of rock socketed pile (II). *Port Waterw. Eng.* 333 (10), 25–27. doi:10.4028/www.scientific.net/AMR.446-449.1387

Chen, C., Leng, W. M., Yang, Y., Jin, Z. H., Nie, R. S., and Qiu, J. (2018). Experimental study of mechanical properties of concrete pile-slurry-sand interface. *Rock Soil Mech.* 39 (7), 2461–2472. doi:10.16285/j.rsm.2017.2219

Cui, Y. W., and Xu, Z. J. (2023). Vertical bearing capacity of pile foundation with reduced diameter cap and deformation of soil around the pile. *J. Henan Univ. Sci. Technol.* 44 (02), 73–79.

Fang, T., Huang, M., and Tang, K. (2020). Cross-section piles in transparent soil under different dimensional conditions subjected to vertical load: an experimental study. *Arab. J. Geosci.* 13, 1133. doi:10.1007/s12517-020-06136-6

FHWA (1998). *Load and resistance factor design for highway bridge substructures*. Washington, DC: Federal Highway Administration, U.S. Department of Transportation. Publication No. FHWA HI-98-032.

Fu, W. Q., Guo, X. G., Chen, Y. Q., and Li, P. J. (2015). Effect of bottom toe debris on the bearing capacity of bored cast-in-place pile. *J. Xiangtan Univ. Nat. Sci. Ed.* 37 (2), 53–60.

Guan, Z. H., and Sun, R. Y. (2021). Numerical simulation of effect of pile bottom sediment on load bearing characteristics of single pile in sandy stratum. *Jiangsu Archit.* 1, 105–107.

Hu, X. F., Gu, L. Y., and Zhang, P. (2014). Analysis and control measures of sediment thickness at hole bottom of bored pile. *Construction* 11, 69–70.

Huang, W. Y. (2018). Study on effect of pile bottom toe debris on mechanical properties of cast-in-place pile. *China Energy Environ. Prot.* 40 (4), 62–67.

Ji, J., Wang, Z., Zhang, Z., and Liao, W. (2023). Robust reliability-based design approach by inverse FORM with adaptive conjugate search algorithm. *Int. J. Numer. Anal. Methods Geomechanics* 47, 1481–1495. doi:10.1002/nag.3524

Ji, J., Zhang, C., Gao, Y., and Kodikara, J. (2019). Reliability-based design for geotechnical engineering: an inverse FORM approach for practice. *Comput. Geotechnics* 111, 22–29. doi:10.1016/j.compgeo.2019.02.027

Jiang, J. P., Wang, M. W., and Gao, G. Y. (2004). Contrastive study on effect of difference of pile end rock-soil layer on super-long pile. *Chin. J. Rock Mech. Eng.* 23 (18), 3190–3195. doi:10.3321/j.issn:1000-6915.2004.18.029

Kou, H. L., Guo, W., Zhang, M. Y., and Xu, Y. Q. (2016). Axial resistance of long rock-socketed bored piles in stratified soils. *Ocean. Eng.* 114, 58–65. doi:10.1016/j.oceaneng.2016.01.013

Li, D. J., Shi, C., Ruan, H. N., Li, B., Li, W., and Yao, X. (2022). Study on shear behavior of coral reef limestone–concrete interface. *Mar. Georesources Geotechnol.* 40 (4), 438–447. doi:10.1080/1064119x.2021.1906365

Li, D. Q., and Yan, L. L. (2008). Reliability analysis method for cast-in-place piles considering pile bottom toe debris. *Soil Mech.* 1, 155–160.

Li, Y. H., Wang, W. D., Huang, M. S., and Guo, Y. C. (2015). Experimental study on pile-soil interface shear of overlong poured pile. *Rock Soil Mech.* 36 (7), 1981–1988. doi:10.16285/j.rsm.2015.07.020

Poulos, H. G. (2005). Pile behavior—consequences of geological and construction imperfections. *J. Geotechnical Geoenvironmental Eng.* 131 (5), 538–563. doi:10.1061/(asce)1090-0241(2005)131:5(538)

Qi, L., and Yu, Y. (2015). An analysis of the effect of slurry skin of the bored piles and improvement measures. *China Rural Water Hydropower* 6, 133–138.

Qian, D. L. (2004). Research on foundation interaction and finite element method simulation. *China Civ. Eng. J.* 2, 82–86. doi:10.3321/j.issn:1000-131X.2004.02.015

Qian, Y., Liu, J., Wang, R., and Jin, Y. (2020a). Experimental study on influence of disc position on soil failure state of expanded pile under horizontal force in oceanographic engineering. *J. Coast. Res.* 108 (1), 274–282. doi:10.2112/jcr-si108-056.1

Qian, Y., Zhou, T., and Tian, W. (2020b). Anti-Overturning Bearing capacity of rigid and flexible concrete expanded piles subjected to horizontal load. *Adv. Civ. Eng.* 4901069, 1–14. doi:10.1155/2020/4901069

Samman, M., and O'Neill, M. W. (1997). The reliability of sonic testing of drilled shafts. *Concr. Int.* 19 (1), 49–54.

Wang, C. H., and An, J. G. (2011). A nonlinear numerical analysis of vertical bearing behavior of bored pile foundations including defective piles with stem shrinkage. *Adv. Mater. Res.* 374–377, 2071–2077. doi:10.4028/www.scientific.net/amr.374-377.2071

Wang, C. H., Li, Q. H., and Zhang, M. N. (2014). Field model test study on vertical bearing behavior of several defective single piles. *Rock soil Mech.* 35 (11), 3207–3230. (in Chinese).

Wong, Y. W. (2004). *Behaviors of large diameter bored pile groups with defects*. China: Hong Kong University of Science and Technology. Masteral Thesis.

Wu, L. C., and Wang, W. (2009). Experimental study on effect of pile bottom sediment on bearing capacity of bored pile. *Eng. Surv.* 2, 351–355.

Wu, Y. J. (2010). Effect of the mud thickness around cast-in-place piles upon the bearing capacity of single pile. *J. Jilin Jian Zhu Univ.* 6, 16–18.

Xu, Z. J., Wang, Z. Q., and Wang, Y. T. (2022). Reliability analysis of bearing capacity of reduced diameter pile based on support vector machine. *J. Earth Sci.*, 1–13.

Yang, G. L., Chen, S. H., and Lin, Y. L. (2009). Comparative experimental study on pile. *J. Railw. Sci. Eng.* 6 (2), 34–37. doi:10.3969/j.issn.1672-7029.2009.02.007

Yang, Y. L. (2011). *Numerical simulations and experimental studies of the effects of mud cake on the vertical bearing behavior of bored piles*. China: Tianjin University. Masteral Thesis.

Yu, X. M., Pan, J., and Yang, N. H. (2006). Analysis of effect of pile bottom sediment and surrounding mud on vertical bearing capacity of large diameter bored pile. *Min. Metallurgy Eng.* 6, 9–12.

Yuan, F., Li, Z. Q., Zhang, J., and Xu, Z. J. (2018). Research of the effects of bottom toe debris on the vertical bearing behavior of end bearing piles. *Henan Sci. Technol.* 634 (3), 114–117.

Zhang, H., and Qian, D. L. (2005a). Reliability analysis of vertical bearing capacity of single pile with squeezed branches and plates. *J. Rock Mech. Eng.* 22, 4197–4201.

Zhang, J. G. (2005b). The analysis and treatment of the stem shrinkage defects in bored piles. *Tunn. Constr.* 25 (4), 21–23,26.

Zhang, L. M., Li, D. Q., and Tang, W. H. (2005c). Impact of routine quality assurance on reliability of bored piles. *J. Geotechnical Geoenvironmental Eng.* 132 (5), 622–630. doi:10.1061/(asce)1090-0241(2006)132:5(622)

Zhang, Q. Q., Zhang, Z. M., and Li, S. C. (2013). Investigation into skin friction of bored pile including influence of soil strength at pile base. *Mar. Georesour. Geotechnol.* 31 (1), 1–16. doi:10.1080/1064119x.2011.626506

Zhang, Y. G., Tian, H. W., and Sun, L. B. (2022). Effect of mud skin on side friction of rotary excavation cast-in-place pile. *Build. Technol. Dev.* 49 (23), 188–190.

Zhang, Z. M., Zhang, G. X., and Wu, Q. Y. (2006). Studies on characteristics of mud cake and soil between bored piles Chinese. *J. Geotechnical Eng.* 6, 695–699.

Zheng, J. J., Xu, Z. J., and Liu, Y. (2010). Reliability analysis of vertical bearing capacity of foundation piles based on maximum entropy principle. *Chin. J. Geotechnical Eng.* 32 (11), 1643–1647.

Zheng, Y. D., and Zheng, R. Y. (2018). Model test study on uplift bearing characteristics of expanded pile. *J. Waterw. Harb.* 39 (02).

Zhou, D. Q., Li, J., and Liu, H. L. (2020). Model test study on compression characteristics of composite foundation with defective piles. *J. Build. Struct.* 41 (07), 131–139.

Zhou, H. B. (2007). Numerical simulation of effects of mud cake and bottom sediment on bearing capacity of bored pile. *Rock Soil Mech.* 28 (5), 956–960.